THE JOURNAL OF PHYSICAL CHEMISTRY B

Article

pubs.acs.org/JPCB

High Ionic Liquid Concentration-Induced Structural Change of Protein in Aqueous Solution: A Case Study of Lysozyme

Takahiro Takekiyo,*[,†] Kumiko Yamazaki,[†] Erika Yamaguchi,[†] Hiroshi Abe,[‡] and Yukihiro Yoshimura[†]

[†]Department of Applied Chemistry, and [‡]Department of Materials Science and Engineering, National Defense Academy, 1-10-20, Hashirimizu, Yokosuka, Japan 239-8686

ABSTRACT: The structural change of chicken egg white lysozyme in aqueous 1-butyl-3-methylimidazolium nitrate ([bmim][NO_3]) solutions (0−24 M) has been investigated by optical spectroscopy and small-angle X-ray scattering (SAXS) methods. Fourier-transform infrared (FTIR) and circular dichroism (CD) spectra and SAXS profiles indicated that the addition of up to 6 M of [bmim][NO_3] induces unfolding of lysozyme resulting from disruption of the α-helix by the NO_3^- ion. On the other hand, even with the addition of more than 10 M of [bmim][NO_3], lysozyme aggregation is inhibited and the protein adopts a partially globular state (the secondary structure is partially refolded while the tertiary structure is disrupted). Observation of the structural features of the aqueous [bmim][NO_3] solution by Raman OD stretching spectra indicated that bulk-like water still remains at concentrations above 10 M and form an "aggregated water" (water pool) in the nanoheterogeneous structure consisting of a polar domain (the high charge-density region) and nonpolar areas (the alkyl-chain region) in the IL. At these concentrations (above 10 M), lysozyme is not sufficiently hydrated because of the reduced number of water molecules. Consequently lysozyme above 10 M assumes the partially globular state. We propose that the changes of the unique IL solution structure (nanoheterogeneous) between the lower and higher [bmim][NO_3] concentrations strongly correlated to the differences in the protein stability of the present results.

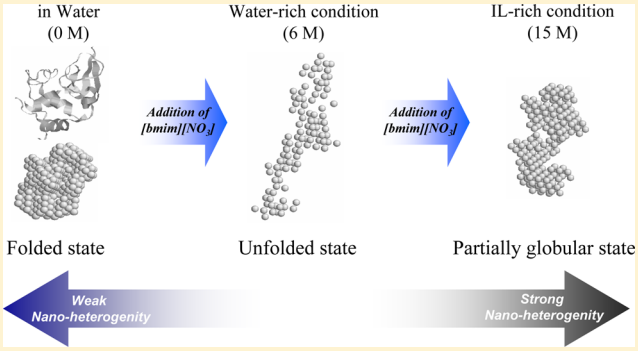

1. INTRODUCTION

Ionic liquids (ILs) comprising a cation and an anion have shown unique physical and chemical properties such as negligible vapor pressure, nonflammability, high chemical/thermal stability, high conductivity, and high solubility for other liquids. They have been widely adopted in various fields, including synthetic chemistry, electrochemistry, and chemical sensing.[1−3]

Recently, the use of ILs in bioscience fields has focused on applications in biotechnology such as biocatalysis and protein storage because ILs provide not only a novel and highly efficient reaction medium but also serve as effective participants in various biological processes.[4−6] Thus, the structural stability and activity of proteins in aqueous IL solutions have been investigated to determine the effect of ILs on biological reaction processes. According to recent studies, aqueous IL solutions increase the protein activity[7−9] and protein stability,[9,10] improve refolding,[11−15] and inhibit aggregation.[16] Lange et al.[11] demonstrated that addition of imidazolium-based ILs (up to 4 M) to the renaturation buffer caused high protein renaturation without the protein aggregation, whereas addition to the folded protein induced the decrease of structural stability in this way. Interactions between ILs and proteins in aqueous solutions are not well understood, and the underlying interpretations are still mostly speculative, although IL−protein interactions within aqueous solutions have been defined for a Hofmeister seires.[17−23] This series ranks the relative influence of ions on the physical behavior of a wide variety of aqueous processes ranging from colloidal assembly to protein folding. Originally, it was thought that an ion's influence on protein folding was caused at least in part by "making" and "breaking" bulk water structure.

Regarding the intriguing features of the aqueous IL solutions, Weingärter et al.[24] reported that the solvent properties of ILs change drastically at a certain IL concentration from typical electrolyte solution-like behavior to molten salt-like behavior depending on the content of water in the mixtures. Actually, the IL−water mixtures showed complicated phase transition[25] along with double glass transition phenomena at 77 K.[26] These behaviors were strongly related to changes in the solution structure of the IL−water mixtures. On the basis of these results, it can be inferred that the changes in the IL concentrations caused the differences in protein stability in these aqueous IL solutions. An understanding of the features contributing to protein stability over a wide IL concentration range in aqueous ILs is necessary to investigate the relationship between solution structure and the stability of protein in these media.

Received: June 11, 2012
Revised: August 13, 2012
Published: August 23, 2012

In this study, we have investigated the structural stability of chicken egg white lysozyme in aqueous [bmim][NO_3] solutions over a broad IL concentration range (0−24 M) using optical spectroscopy (FTIR, CD, and Raman) combined with small-angle X-ray scattering (SAXS) methods. Lysozyme is commonly used for studying the structural stability of proteins in aqueous IL solutions.[27,28] 1-Butyl-3-methylimidazolium nitrate ([bmim][NO_3]) is low-melting and highly water-soluble. Our results demonstrated that the addition of [bmim][NO_3] above 6−10 M inhibits the aggregation of lysozyme and induces the protein to take on a partially globular state, whereas the addition of [bmim][NO_3] up to 6 M induces the unfolding of lysozyme. We interpret the difference in protein stability between the lower and higher [bmim][NO_3] concentrations as a strong correlation ion with changes in the solution structure of the aqueous IL solutions.

2. MATERIALS AND METHODS

Chicken egg white lysozyme (Wako Junyaku Co.) was used without further purification, and 1-butyl-3-methylimidazolium nitrate ([bmim][NO_3], Sigma) was used as IL. The concentration of water in [bmim][NO_3] as-received samples was determined and verified to be 130−150 ppm using the Karl Fischer titration method. All of the mixtures of different concentrations (0−24 M) were prepared by mixing the required amount of [bmim][NO_3] and D_2O (99.9%, Aldrich Co.). Sample preparation was done in a drybox to avoid atmospheric H_2O and CO_2. For all spectral measurements, the protein concentration was adjusted to 1.0 mM (0−24 M and pD 2.0−4.5) as determined spectrophotometrically using the ultraviolet absorbance at 280 nm. The pD values were estimated by adding 0.4 to the read value taken from a pH meter.[29] The sample was loaded into a cell with CaF_2 windows and a 100-μm Teflon spacer for FTIR and CD spectral measurements. FTIR and CD spectra could not be acquired for the protein solutions having around 1−2 M [bmim][NO_3] owing to the salting-out phenomenon.

FTIR spectra were recorded using a Nicolet 6700 FTIR spectrometer equipped with an MCT liquid-nitrogen-cooled detector. Typically, 512 interferograms were collected to obtain a spectrum with the resolution of 4 cm^{-1}. All exchangeable backbone amide protons were deuterated by incubating the protein in a D_2O solution during 1 day. Completion of hydrogen−deuterium exchange was confirmed by the cessation of shifts in the amide II band. This band, in the frequency region around 1550 cm^{-1}, is known to shift to approximately 1450 cm^{-1} on deuteration of the backbone amide protons. Solvent spectra were also measured under the same conditions as those used for the protein solution measurements, and they were subtracted from the protein solution spectra.

CD spectra were measured over the wavelength range from 250 to 300 nm on a JASCO J-820 spectopolarimeter. It is well-known that far-UV CD spectroscopy is a powerful tools for investigating changes in the secondary structures of peptides and proteins.[30−32] However, we could not observe the far-UV CD spectrum of lysozyme below 250 nm because of the strong peak of the imidazolium ring in the $[bmim]^+$ cation.[33] Typical spectra were accumulated at the scan rate of 20 nm/min with a 0.1-nm step. Five scans were averaged for each spectrum. The obtained spectra were converted to mean residue ellipticity units using $[\theta] = \theta_{obs}/(10ncl)$, where θ_{obs} is the observed ellipticity, l is the path length, c is the concentration of lysozyme, and n is the number of residues.

Raman spectra were measured by a JASCO NR-1800 Raman spectrophotometer equipped with a single monochromator and a charge coupled device detector. The exposure time for each run and spectral resolution were 300 s and 4.5 cm^{-1}, respectively. The 514.5-nm line from a Lexel Ar^+ ion laser was used as the excitation source at the power of 200 mW. All IR and Raman spectral analyses were performed using GRAMS Research tm (Galactic Software).

SAXS experiments were carried out using a Kratky camera system (BioSAXS-1000, Rigaku Co.) at the brilliance of 56.0 kW/mm^2. Cu Kα radiation (λ = 0.1542 nm) was selected and collimated using a parabolic multilayer mirror. Further, the beam was focused by a converting optical tool (CBO-*f*, Rigaku Co.). The beam size was 0.5 mm (V) × 0.1 mm (H) at the sample position, and the camera length was 500 mm. The combination of the 2D Kratky block and focusing optics can achieve a wide q range. Here the scattering vector q, is defined as $4\pi(\sin\theta)/\lambda$ (nm^{-1}). All assemblies were set inside the vacuum chamber to remove air scattering. A 2D detector (PILATUS 100K/R) was used. Samples were put into quartz capillaries with a diameter of 1.0 mm and thickness of 0.1 mm. Sample volumes was 5−30 μL. The radius of gyration (R_g) value was obtained from the slope of the Guinier plot ($\ln I(q)$ vs q^2) from low q regions of the solution scattering curve.[34] The scattering of the aqueous [bmim][NO_3] solution was subtracted, and the final scattering curve was obtained using the program *PRIMUS*.[35]

3. RESULTS AND DISCUSSION

3.1. Structural Changes of Lysozyme in the Aqueous [bmim][NO_3] Solutions. Figure 1a shows FTIR spectra of the amide I′ region of lysozyme in the aqueous [bmim][NO_3] solutions at several concentration of [bmim][NO_3] (0−24 M). The amide I′ (the deuterated peptide groups) vibrational mode in the FTIR spectrum is highly sensitive to the secondary structures of proteins, and thus it serves as an indicator of α-helix and/or β-sheet formation.[36−38] From Figure 1a, the amide I′ spectra of lysozyme changed significantly as a function of the [bmim][NO_3] concentration. The decrease in absorbance at 1654 cm^{-1} ($Abs_{1654\ cm\text{-}1}$) (●) indicating disruption of the secondary structure was observed at IL concentrations of up to 6 M as shown in Figure 1b. On the other hand, it is remarkable that the value of $Abs_{1654\ cm\text{-}1}$ increased again in the region from 6 to 10 M and became constant above 10 M. This result suggests the partial refolding of the secondary structure of lysozyme.

Next we measured the changes in the tertiary structure of lysozyme induced by the [bmim][NO_3] using CD spectroscopy (data not shown). The near-UV CD spectrum in the region from 250 to 300 nm is sensitive to the presence of specific rigid packing interactions of the aromatic side-chains, indicating a change in the tertiary structure.[39] As shown in Figure 1b, although the positive CD intensity (○) at 292 nm because of the aromatic residues drastically decreased at IL concentrations of up to 5 M, the increment of the positive CD intensity did not occur above 5 M. This means that the increase in the [bmim][NO_3] concentration completely disrupted the tertiary structure of lysozyme above 5 M.

The results from the FTIR and CD spectra showed that the aqueous solutions of up to ∼6 M of [bmim][NO_3] caused lysozyme to unfold. Most of the previous experimental results pointed out that dilute aqueous imidazolium-based solutions (less than 5 M) induced protein unfolding.[16−19] The present

dx.doi.org/10.1021/jp3057064 | J. Phys. Chem. B 2012, 116, 11092−11097

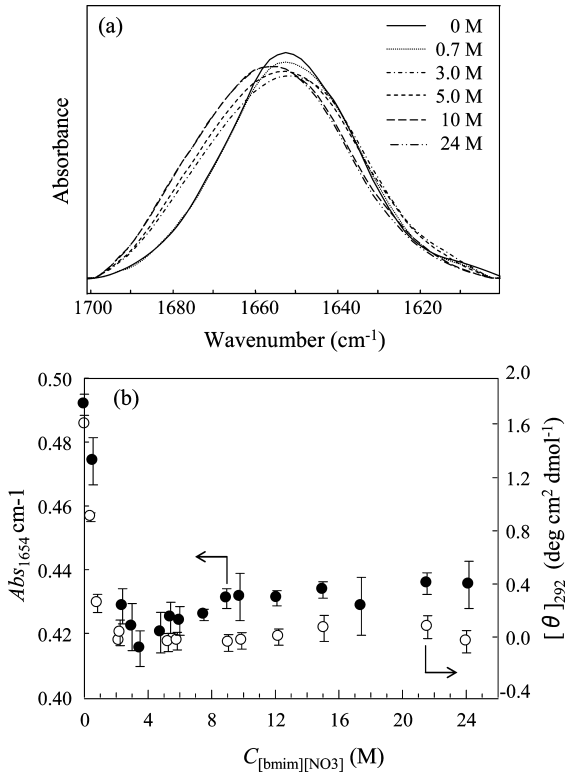

Figure 1. (a) FTIR spectra in the amide I′ region of lysozyme in the aqueous [bmim][NO_3] solutions at several concentration of [bmim][NO_3]. (b) Changes in the absorbance at 1654 cm^{-1} ($Abs_{1654\ cm\text{-}1}$) (●) and molar ellipticity at 292 nm ($[\theta]_{292}$) (○) of lysozyme as a function of [bmim][NO_3] concentration.

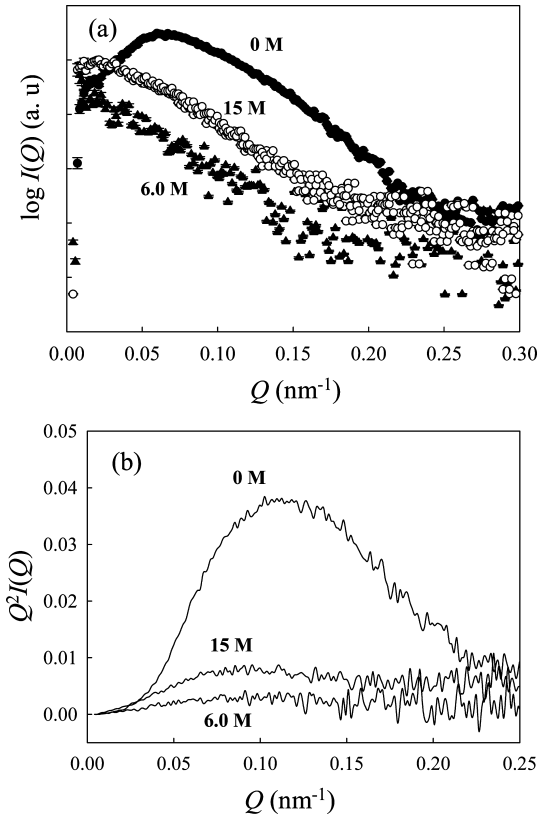

Figure 2. (a) SAXS profiles of lysozyme in the aqueous [bmim][NO_3] solutions at 0 M (●), 6 M (▲), and 15 M (○). (b) The Kratky plots of lysozyme in the aqueous [bmim][NO_3] solutions at 0, 6, and 15 M.

result showing similar changes up to 6 M is in agreement with these previous conclusions. On the other hand, the changes in secondary structure indicated by the FTIR spectra of solutions above 6 M showed a behavior different from that of the tertiary structure observed by CD. Thus, the secondary structure of lysozyme seems to be partially refolded in the 6−10 M concentration range, whereas the tertiary structure breaks down. Regarding the control of protein refolding by imidazolium-based ILs, Lange et al.[11] and Buchfink et al.[12] showed that these species promote the renaturation of proteins by suppressing aggregation. On the other hand, small-angle neutron scattering (SANS) results obtained by Heller and Baker indicated that protein aggregated at higher imidazolium-based IL concentrations.[18,19] Here, in an effort to determine whether lysozyme aggregates above 6 M, we measured SAXS profile of lysozyme in aqueous [bmim][NO_3] solutions. The SAXS method is a powerful technique for investigating protein size and the presence of protein aggregation.[40,41]

Figure 2a shows the SAXS curve of $I(q)$ vs q, for lysozyme in aqueous [bmim][NO_3] solutions at 0, 6, and 15 M. The SAXS curve of lysozyme at 0 M showed a typical folded state, which is consistent with a previous SAXS profile of lysozyme.[34] It appeared that lysozyme in the aqueous [bmim][NO_3] solutions at 6 and 15 M also did not aggregate because the corresponding SAXS curves did not show a drastic increase in $I(q)$ below q − 0.03, which is generally indicative of protein aggregation. The radius of gyration (R_g) values for lysozyme obtained by the Guiner analysis are predictive of protein size and are estimated to be 1.40 ± 0.07, 2.38 ± 0.08, and 1.91 ± 0.03 nm for 0, 6, and 15 M solutions, respectively. The R_g values at 0 and 6 M are in good agreement with those of the folded state and 4 M GdnHCl-induced unfolded state reported by Hoshino et al.[41] Thus, lysozyme in the aqueous [bmim][NO_3] solutions at 0 and 6 M adopts the folded and unfolded states, respectively. Interestingly, the R_g value of lysozyme in the 15 M solution is larger than that at 0 M and smaller than that at 6 M. Thus, lysozyme at 15 M takes a more compact structure than that at 6 M and did not completely unfold.

A similar result was also obtained by Kratky plots, as shown in Figure 2b. The presence of a peak in the Kratky plot is a clear indication that a globular protein state was successfully achieved because the curve for an expanded unfolded conformation would be expected to show a plateau.[43,44] The Kratky plots of lysozyme at 0 and 6 M concentrations of [bmim][NO_3] showed typical globular and unfolded states, respectively. It is remarkable that this plot of lysozyme at 15 M had a small peak, which indicated that the protein existed in a partially globular state. The R_g values and Kratky plot showed that the structure of lysozyme at 15 M adopts the intermediate state, which is partially globular (between the globular and unfolded states). These results are highly consistent with the changes in the secondary structure suggested by FTIR spectroscopy. FTIR, CD, and SAXS results all showed that lysozyme in the aqueous [bmim][NO_3] solutions takes on the unfolded state below 6 M and the partially globular disrupted tertiary structure above 10 M. Consequently, changes in the concentration of [bmim][NO_3] induced structural transitions of the folded state → unfolded state → partial globular state.

3.2. Relationship between the Structural Stability of Lysozyme and the Solution Structure in the Aqueous [bmim][NO_3] Solutions. Lysozyme structural changes in

dx.doi.org/10.1021/jp3057064 | J. Phys. Chem. B 2012, 116, 11092−11097

aqueous [bmim][NO_3] solutions have been investigated using FTIR and CD spectroscopy combined with SAXS. Our results showed that the lysozyme structure adopts the unfolded state below 6 M and the partially globular state above 10 M. In an effort to understand the origin of these effects, we focused on the relationship between the secondary structure of lysozyme and the structure of the aqueous [bmim][NO_3] solutions.

First, we determined the area fractions (f) of each secondary structure to evaluate the detailed changes in the secondary structure of lysozyme by the curve-fitting method. Figure 3a shows the curve-fitted FTIR spectrum of the amide I′ region of lysozyme in aqueous solution (0 M). Five peaks in the spectrum of lysozyme at 0 M, which are 1609, 1633, 1643, 1654, and 1670 cm^{-1}, correspond to the side-chain (Tyr residue), β-sheet, disordered structure, α-helix, and turn structures, respectively.[36,37] The area fractions (f) of the secondary structure of lysozyme (0 M) are 0.2 for the β-sheet, 0.12 for the disordered structure, 0.48 for the α-helix, and 0.2 for the turn structures, respectively. These values are consistent with those found previously.[36]

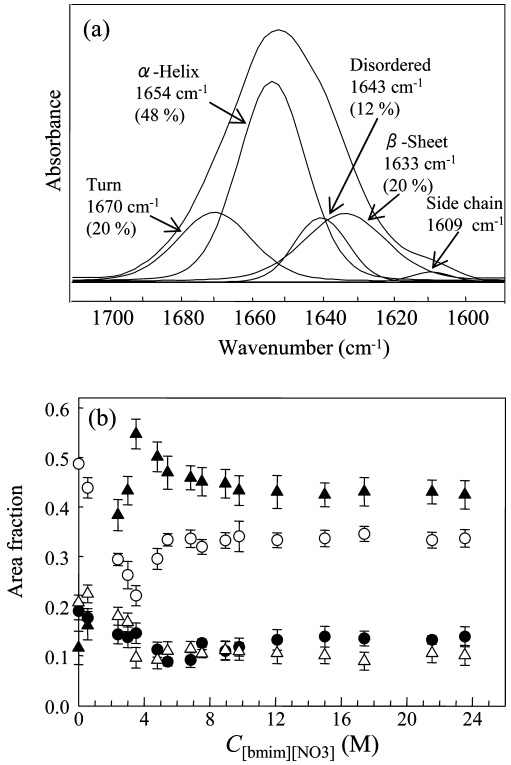

Figure 3. (a) Result of the curve-fitting of the amide I′ spectrum of lysozyme in water. (b) Concentration dependence of the area fractions (f) for the amide I′ component of the secondary structures. The estimation of f used the relationship $f^{\alpha\text{-Helix}} = I^{\alpha\text{-Helix}}/(I^{\beta\text{-sheet}} + I^{\text{Disordered}} + I^{\alpha\text{-Helix}} + I^{\text{turn}})$, where I is the integrated intensities of the peaks at β-sheet (1633 cm^{-1}), disordered structure (1643 cm^{-1}), α-helix (1654 cm^{-1}), and turn (1670 cm^{-1}) structures, respectively. The symbols, which are ○, ●, △, and ▲, represent the α-helix, β-sheet, turn, and disordered structures, respectively.

Figure 3b shows the changes in the f values for the secondary structure of lysozyme as a function of [bmim][NO_3] concentration. The f values of the α-helix and β-sheet structures decrease with increasing [bmim][NO_3] concentration (up to 6 M), and that of the disordered structure increases. On the other hand, with further increase in the [bmim][NO_3] concentration (up to 10 M), the f values of the α-helix and β-sheet structures again increase, and that of the disordered structure decreases. The reformation of the α-helix and β-sheet structures in the 6–10 M solutions (formation of the partial globular state) are approximately 30% and 10%, respectively. The higher [bmim][NO_3] concentration above 6 M induced the reformation of α-helix structure of the unfolded lysozyme. The present result shows a similar behavior with the alcohol denaturation of proteins. The nonaqueous environment of alcohols such as trifluoroethanol (TFE) and methanol is known to increase significantly the α-helical content of many proteins.[42,45−50] According to the CD and SAXS results by Hoshino et al.,[42] the addition of TFE above 15 v/v % (~2 M) to the folded lysozyme induced the increase of the α-helical structure. Interestingly, R_g value (2.10 ± 0.6 nm) of lysozyme in the 40 v/v % TFE (~5.5 M) is close to that in the 15 M [bmim][NO_3] (1.91 ± 0.03 nm).[42] Although IL and alcohol solutions induce the increase of α-helix structure of lysozyme, the concentrations showing the increase of α-helix structure are different from each other. Thus, although the effect of addition of [bmim][NO_3] on structural stability of proteins may show the similar analogy with alcohol, it is difficult to say more about the details.

Next we focused on the solution structure of aqueous [bmim][NO_3] solutions. Small- and wide-angle X-ray scattering (SWAXS) and MD simulations results showed that the solution structure of imidazolium-based ILs forms a nanostructural organization (nanoheterogeneous structure) consisting of a polar domain (imidazolium ring and anion) and a nonpolar domain (alkyl-chain of the cation).[51−55] Importantly, there is a nanophase separation structure but no macroscopic phase separation occurs. Interestingly, recent MD simulation results by Jiang et al.[54] showed that the imidazolium-based IL−water mixtures under water-rich conditions (~6 M) adopts an the imidazolium-based IL aggregate structure surrounded by bulk water, and the nanoheterogeneity is low. However, under IL-rich conditions (~10 M), the water molecules are scattered on the polar domain and form an "aggregated water"[54,56] (hereafter, we denoted these water molecules as "water pool") in the imidazolium-based IL. Thus, the solution structure under the water-rich conditions is different from that presents under IL-rich conditions. From this relation, we presume that the [bmim][NO_3] concentration-dependent changes in the lysozyme structure correlate with the changes in the nanoheterogeneous structure of the aqueous [bmim][NO_3] solutions.

To assess this speculation, we acquired Raman OD stretching (ν_{OD}) spectra, which are highly sensitive to intermolecular hydrogen bonding among water molecules, in the aqueous [bmim][NO_3] solutions (a) without lysozyme and (b) with lysozyme, as shown in Figure 4. Overall, the Raman ν_{OD} spectra changed with the addition of [bmim][NO_3], as shown in Figure 4a. The Raman intensity at ~2380 cm^{-1} because of the bulk-like water[57,58] drastically decreased with increasing [bmim][NO_3] concentration, and that at ~2500 cm^{-1} corresponding to the D_2O hydrated anion[57,58] increased up to 6 M. Further addition of [bmim][NO_3], changes in the Raman ν_{OD} intensities at ~2380 and ~2500 cm^{-1} become smaller. These results mean that the solution structure in the aqueous [bmim][NO_3] solution below 6 M is different from that above 6 M.

Similar results by the addition of [bmim][NO_3] were also obtained in the Raman ν_{OD} frequency shifts at ~2380 and ~2500 cm^{-1}. Figure 5 shows the frequency shifts of two peaks

dx.doi.org/10.1021/jp3057064 | J. Phys. Chem. B 2012, 116, 11092−11097

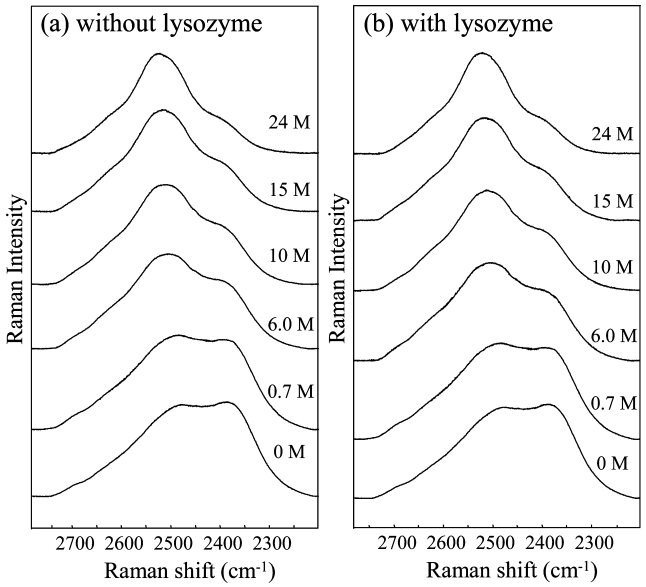

Figure 4. Raman spectra of OD stretching region in the aqueous [bmim][NO_3] solutions as a function of [bmim][NO_3] concentration (a) without lysozyme and (b) with lysozyme.

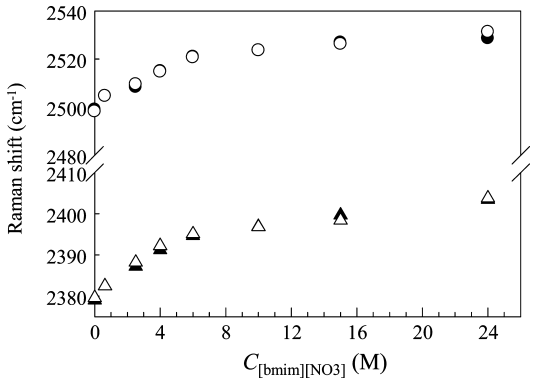

Figure 5. Changes in the Raman OD stretching frequencies at ~2380 (triangle) and ~2500 cm^{-1} (circle) in the aqueous [bmim][NO_3] solutions as a function of [bmim][NO_3] concentration. The closed and open symbols represent the frequency shifts without lysozyme and with lysozyme, respectively.

(~2380 and ~2500 cm^{-1}) of aqueous [bmim][NO_3] solution as a function of [bmim][NO_3] concentration. Both peaks shift to higher frequency up to 6 M due to the change from the hydrogen bonds between the D_2O molecules to those between D_2O−IL. On the other hand, higher frequency shifts become smaller above 6 M. It is remarkable that the peak at ~2380 cm^{-1} still remains at 24 M. Although Raman spectra are not so sensitive to nanoheterogeneous structural change as SAXS, the present Raman spectral change occurred at the similar IL concentration region showing the solution structure change reported by the results of MD simulation.[54] On the basis of above results, we suggest that water molecules form the "water pool" site in the nanoheterogeneous structure even at high [bmim][NO_3] concentrations.

Also remarkable, the Raman spectral changes induced by the addition of [bmim][NO_3] are independent of the presence of lysozyme, as shown in Figures 4b and 5, or not observed throughout the studied concentrations. Consequently, the nanoheterogeneity of the aqueous [bmim][NO_3] solutions hardly change on addition of lysozyme.

On the basis of the protein structure and solution structure results, we have developed a plausible mechanism for the structural changes of lysozyme in the aqueous [bmim][NO_3] solutions. A recent optical spectroscopic study pointed out that the NO_3^- anion in dilute aqueous [bmim][NO_3] solutions interacts strongly with the protein and enters its interior thereby disrupting essential intraprotein hydrogen bonds, those in the α-helix region.[59] In the present FTIR result, the α-helix of lysozyme drastically decreased as the IL concentration increased up to 6 M. Similar results were also obtained by FTIR spectral analysis of lysozyme in the aqueous $LiNO_3$ and tetramethylammonium nitrate (Me_4NNO_3) solutions (data not shown). In the both salts solutions, the α-helix of lysozyme decreased with increasing concentrations of $LiNO_3$ and Me_4NNO_3 up to 10 M, though the degree of disruption of α-helix is dependent on the cationic species. Furthermore, the Raman ν_{OD} spectra indicated that the motional freedom of the cation and anion are high up to 6 M owing to the bulk-like water. On the basis of these results, it can be suggested that lysozyme in the 6 M solution unfolds as a results of disruption of the α-helix by the NO_3^- anion. On the other hand, above 10 M, the motional freedom of cation and anion is more limited than when the concentration is below 6 M, where water molecules form the "water pool" site in the nanoheterogeneous structure. Lysozyme selectively interacts with water molecules in the "water pool" site. However, lysozyme is not sufficiently hydrated because of the reduced number of water molecules. Therefore, lysozyme adopts a partially globular state.

On the basis of the above results, we proposed that protein stability in the aqueous IL solutions is correlated with the changes in the solution structure (nanoheterogeneous structure) of the aqueous IL solutions. As mentioned in the introduction, some aqueous IL solutions (up to ~4 M) improve refolding,[11−15] and inhibit aggregation.[16] Interestingly, our results demonstrated that change in the concentration of [bmim][NO_3] induced the inhibition of lysozyme aggregation where we detect the process of the unfolded state → partial globular state of lysozyme. Unfortunately, it is difficult to say more about the details of the partial globular state of lysozyme. More continuous experimental studies such as thermodynamic and kinetic analyses will give us further knowledge for understanding the partial globular state above 6.0 M of lysozyme.

4. CONCLUSION

Structural changes of lysozyme in aqueous [bmim][NO_3] solutions have been investigated using optical spectroscopy and SAXS methods. We found that lysozyme adopts the unfolded state at IL concentrations up to 6 M but the folded state resurrects above 10 M forming a partially globular state which disrupted tertiary structure. Furthermore, the structural changes of lysozyme in aqueous [bmim][NO_3] solutions correlate to the changes in the solution structure (nanoheterogeneous) of the medium consisting of IL and water. In other words, changes in the nanoheterogeneity control protein stability.

As another interesting result, Yoshimura et al.[26,60] showed that aqueous imidazolium-based IL solutions demonstrated significant glass formation at concentrations >6 M (77 K). Interestingly, the glass forming concentration region of the aqueous IL solutions is consistent with the concentration associated with the partially globular state of lysozyme. A

dx.doi.org/10.1021/jp3057064 | J. Phys. Chem. B 2012, 116, 11092−11097

possible application of the present study for future investigation such as the measurement of protein activity may relate to the potential use for highly aqueous IL solutions as a new cryoprotectant for aqueous biomolecular systems.

AUTHOR INFORMATION

Corresponding Author

*E-mail: take214@nda.ac.jp.

Notes

The authors declare no competing financial interest.

ACKNOWLEDGMENTS

We appreciate Prof. T. Kurotsu, Dr. C. Nakazawa, and Dr. M. Aono of NDA for helpful CD and UV spectral measurements.

REFERENCES

(1) Liu, J. F.; Jonsson, J. A.; Jiang, G. B. *TrAC, Trends Anal. Chem.* **2005**, *24*, 20.
(2) Hallett, J. P.; Welton, T. *Chem. Rev.* **2011**, *111*, 3508.
(3) Faridbod, F.; Ganjali, M. R.; Norouzi, P.; Riahi, S.; Rashedi, H. *In Ionic Liquids: Application of room temperature ionic liquids in electrochemical sensors and biosensors*; Intech Publisher: Croatia, 2011; Chapter 29.
(4) Park, S.; Kazlauskas, R. J. *Curr. Opin. Biotechnol.* **2003**, *14*, 432.
(5) van Rantwijk, F.; Lau, R. M.; Sheldon, R. A. *Trends Biotechmol.* **2003**, *21*, 131.
(6) van Rantwijk, F.; Sheldon, R. A. *Chem. Rev.* **2007**, *107*, 2757.
(7) Dominguez de Maria, P. *Angew. Chem., Int. Ed.* **2008**, *47*, 6960.
(8) Fujita, K.; Ohno, H. *Biopolymers* **2010**, *93*, 1093.
(9) Fujita, K.; MacFarlane, D. R.; Forsyth, M. *Chem. Commun.* **2005**, 4804.
(10) Fujita, K.; MacFarlane, D. R.; Forsyth, M.; Yoshizawa-Fujita, M.; Murata, K.; Nakamura, N.; Ohno, H. *Biomacromolecules* **2007**, *8*, 2080.
(11) Lange, C.; Patil., G.; Rudolph, R. *Protein Sci.* **2005**, *14*, 2693.
(12) Buchfink, R.; Tischer, A.; PAtil., G.; Rudolph, R.; Lange, C. *J. Biotechnol.* **2010**, *150*, 64.
(13) Summers, C. A.; Flowers, R. A. *Protein Sci.* **2000**, *9*, 2001−2008.
(14) Yamaguchi, S.; Yamamoto, E.; Tsukiji, S.; Nagamune, T. *Biotechnol. Prog.* **2008**, *24*, 402.
(15) Byrne, N.; Angell, C. A. *J. Mol. Biol.* **2008**, *378*, 707−714.
(16) Byrne, N.; Wang, L.-M.; Belieres, J.-P.; Angell, C. A. *Chem. Commun.* **2007**, 2714.
(17) Constantinescu, D.; Herrman, C.; Weingärtner, H. *Phys. Chem. Chem. Phys.* **2007**, *12*, 1756.
(18) Constantinescu, D.; Weingärtner, H.; Herrman, C. *Angew. Chem., Int. Ed.* **2007**, *46*, 8887.
(19) Baker, D. A.; Heller, W. T. *Chem. Eng. J.* **2009**, *147*, 6−12.
(20) Heller, W. T.; O'Neill, H. M.; Zhang, Q.; Baker, G. A. *J. Phys. Chem. B* **2010**, *114*, 13866.
(21) Bae, S. Y.; Kim, S.; Lee, B. Y.; Kim, K. K.; Kim, T. D. *Anal. Biochem.* **2011**, *419*, 354.
(22) Zhang, Y.; Cremer, P. S. *Curr. Opin. Chem. Biol.* **2006**, *10*, 658.
(23) Zhao, H.; Olubajo, O.; Song, Z.; Sims, A. L.; Person, T. E.; Lawal, R. A.; Holley, L. A. *Bioorg. Chem.* **2006**, *34*, 15.
(24) Weingärtner, H.; Cabrele, C.; Herrman, C. *Phys. Chem. Chem. Phys.* **2012**, *14*, 415.
(25) Abe, H.; Yoshimura, Y.; Imai, Y.; Goto, T.; Matsumoto, H. *J. Mol. Liq.* **2009**, *150*, 16.
(26) Yoshimura, Y.; Kimura, H.; Okamoto, C.; Miyashita, T.; Imai, Y.; Abe, H. *J. Chem. Thermodyn.* **2011**, *43*, 410.
(27) Cho, T. Y.; Byrne, N.; Moore, D. J.; Pethica, B. A.; Angell, C. A.; Debenedetti, P. G. *Chem. Commun.* **2009**, 4441.
(28) Rodrigues, J. V.; Prosinecki, V.; Marrucho, I.; Rebelo, L. P. N.; Gomes, C. M. *Phys. Chem. Chem. Phys.* **2011**, *13*, 13614.
(29) Kręźl, A.; Bal., W. *J. Inorg. Biochem.* **2004**, *98*, 161.
(30) Greenfield, N.; Fasman, G. D. *Biochemistry* **1969**, *8*, 4108.
(31) Kelly, S. M.; Jess, T. J.; Price, N. C. *Biochim. Biophys. Acta* **2005**, *1751*, 119.
(32) Chen, Y. H.; Yang, J. T.; Chau, K. H. *Biochemistry* **1974**, *13*, 3350.
(33) Paul, A.; Mandal, P. K.; Samata, A. *J. Phys. Chem. B* **2005**, *109*, 9148.
(34) Mylonas, E.; Svergun, D. I. *J. Appl. Crystallogr.* **2007**, *40*, 245.
(35) Konarev, P. V.; Volkov, V. V.; Sokolova, A. V.; Koch, M. H. J.; Svergun, D. I. *J. Appl. Crystallogr.* **2003**, *36*, 1277.
(36) Kong, J.; Yu, S. *Acta Biochim. Biophys. Sin.* **2007**, *38*, 549.
(37) Smeller, L.; Meersman, F.; Heremans, K *Biochim. Biophys. Acta* **2006**, *1764*, 497.
(38) Bandekar, J. *Biochim. Biophys. Acta* **1992**, *1120*, 123.
(39) Mizuguchi, M.; Arai, M.; Ke, Y.; Nitta, K.; Kuwajima, K. *J. Mol. Biol.* **1998**, *283*, 265.
(40) Cinelli, S.; Spinozzi, F.; Itri, R.; Finet, S.; Carsughi, F; Onori, G.; Mariani, P. *Biophys. J.* **2001**, *81*, 3522.
(41) Uzawa, T.; Akiyama, S.; Kimura, T.; Takahashi, S.; Ishimori, K.; Morishima, I.; Fujisawa, T. *Proc. Natl. Acad. Sci. U.S.A.* **2004**, *101*, 1171.
(42) Hoshino, M.; Hagihara, Y.; Hamada, D.; Kataoka, M.; Goto, Y. *FEBS Lett.* **1997**, *416*, 72.
(43) Kataoka, M.; Hagihara, Y.; Mihara, K.; Goto, Y. *J. Mol. Biol.* **1993**, *229*, 591.
(44) Kataoka, M.; Nishii, I.; Fujisawa, T.; Ueki, T.; Tokunaga, F.; Goto, Y. *J. Mol. Biol.* **1995**, *249*, 215.
(45) Shiraki, K.; Nishikawa, K.; Goto, Y. *J. Mol. Biol.* **1995**, *245*, 180.
(46) Hamada, D.; Kuroda, Y.; Tanaka, T.; Goto, Y. *J. Mol. Biol.* **1995**, *254*, 737.
(47) Kamatari, Y. O.; KOnnno, T.; Kataoka, M.; Akasaka, K. *J. Mol. Biol.* **1996**, *259*, 512.
(48) Schönbrunner, N.; Wey, J.; Engels, J.; Georg, H.; Kiefhaber, T. *J. Mol. Biol.* **1996**, *260*, 432.
(49) Hirota, N.; Mizuno, K.; Goto, Y. *J. Mol. Biol.* **1998**, *275*, 365.
(50) Gast, K.; Zirwer, D.; Müller-frohne, M.; Damaschun, G. *Protein Sci.* **1999**, *8*, 625.
(51) Triolo, A.; Russina, O.; Bleif, H.-J.; DiCola, E. *J. Phys. Chem. B* **2006**, *111*, 4641.
(52) Lopes, J. N. A. C.; Pádua, A. A. H. *J. Phys. Chem. B* **2006**, *110*, 3330.
(53) Wang, Y.; Voth, G. A. *J. Phys. Chem. B* **2006**, *110*, 18601.
(54) Jiang, W.; Wang, Y.; Voth, G. A. *J. Phys. Chem. B* **2007**, *111*, 4812.
(55) Bernardes, C. E. S.; Minas da Piedade, M. E.; Lopes, J. N. C. *J. Phys. Chem. B* **2011**, *115*, 2067.
(56) Masaki, T.; Nishikawa, K.; Shirota, H. *J. Phys. Chem. B* **2010**, *114*, 6323.
(57) Zhang, L.; Xu, Z.; Wang, Y.; Li, H. *J. Phys. Chem. B* **2008**, *112*, 6411.
(58) Yoshimura, Y.; Takekiyo, T.; Okamoto, C.; Hatano, N.; Abe, H. Submitted for publication.
(59) Shu, Y.; Liu, M.; Chen, S.; Chen, X.; Wang, J. *J. Phys. Chem. B* **2011**, *115*, 12306.
(60) Imai, Y.; Abe, H.; Miyashita, T.; Goto, T.; Matsumoto, H.; Yoshimura, Y. *Chem. Phys. Lett.* **2010**, *486*, 37.